Density functional study of the overdoped iron chalcogenide TlFe$_2$Se$_2$ with ThCr$_2$Si$_2$ structure

Lijun Zhang and D. J. Singh

Materials Science and Technology Division, Oak Ridge National Laboratory, Oak Ridge, Tennessee 37831-6114, USA
(Received 2 February 2009; published 31 March 2009)

We report density functional calculations of electronic structure and magnetic properties of ternary iron chalcogenide TlFe$_2$Se$_2$, which occurs in the ThCr$_2$Si$_2$ structure and discuss the results in relation to the iron-based superconductors. The ground state is antiferromagnetic with checkerboard order and Fe moment $\sim 1.90 \mu_B$. There is strong magnetoelastic coupling similar to the Fe-based superconductors, reflected in a sensitivity of the Se position to magnetism. Tl is monovalent in this compound, providing heavy electron doping of 0.5 additional carriers per Fe relative to the parent compounds of the Fe-based superconductors. Other than the change in electron count, the electronic structure is rather similar to those materials. In particular, the Fermi surface is closely related to those of the Fe-based superconductors, except that the electron cylinders are larger, and the hole sections are suppressed. This removes the tendency toward a spin-density wave.

I. INTRODUCTION

The finding of superconductivity in layered Fe oxypnictides with the ZrCuSiAs structure[1,2] has stimulated much interest leading to the discovery of many additional compounds with critical temperatures up to ~ 56 K.[3,4] Superconductivity occurs quite generally in these compounds, and is robust against off-site substitutions and variations in the structure, including doped fluoro-arsenides SrFeAsF,[5,6] as well as ThCr$_2$Si$_2$-type arsenides [prototype BaFe$_2$As$_2$ (Ref. 7)], Cu$_2$Sb-structure LiFeAs (Ref. 8), [NaFeAs (Ref. 9)], and PbO-structure Fe(Se,Te).[10,11]

All these materials have square planar Fe^{2+} layers, tetrahedrally coordinated by anions, and are near magnetism. The undoped compounds generally show a spin-density wave (SDW),[12–14] and superconductivity appears when this SDW is suppressed either by pressure or doping. This suggests an involvement of magnetism in the pairing.[15] In addition there is accumulating evidence for strong antiferromagnetic correlations in this family in the normal metallic states, e.g., from the temperature dependence of the susceptibility, which increases with T.[16,17]

As mentioned, the binary chalcogenide α-FeSe is also superconducting when doped by off-stoichiometry.[10] T_c for this material reaches 27 K under pressure,[11] while the electronic structure is very similar to the pnictide phases, according to both density functional calculations[18] and photoemission.[19] Among the chalcogenides, experiments indicated that FeTe might have the strongest superconductivity based on the increase in T_c upon alloying FeSe with Te, (increasing from 8 to 15 K)[20] as well as theoretical considerations based on the strength of its SDW.[18] However, FeTe shows an antiferromagnetic ground state instead of superconductivity,[21–23] which implies additional doping (or pressure) is still required to further suppress magnetism and perhaps induce superconductivity. Modest superconductivity (10 K) has already been observed when alloying FeTe with S.[24] In this regard, it is important to note that α-FeSe and FeTe generally form off-stoichiometry with excess Fe partially filling interstitial sites in the chalcogen layer. This excess Fe acts as an electron dopant, and suppresses SDW order by donating carriers to Fe-Se layers.[25] In addition, the excess Fe carries local magnetic moments that may be expected to interact with spin fluctuations associated with the Fe-Se layers and also produce pair breaking.[22,25,26] Therefore, it is of interest to explore alternate chemical doping strategies for FeSe and FeTe, perhaps based on related compounds.

Here we report density functional studies of TlFe$_2$Se$_2$, which is a ternary iron chalcogenide occurring in ThCr$_2$Si$_2$ structure. Little is known about the physical properties of this compound, except that it has been synthesized and that it has a magnetic transition at ~ 450 K, as observed in Mössbauer measurements. The magnetic state was characterized as antiferromagnetic based on the lack of attraction of the magnetic phase by a magnet.[27]

II. STRUCTURE AND METHODS

From a structural point of view, TlFe$_2$Se$_2$ (Fig. 1) is closely related to FeSe, and in particular consists of practically identical Fe-Se layers, consisting of edge-sharing FeSe$_4$ tetrahedra, although these are now intercalated with Tl, altering the stacking sequence. The large size of Tl cations (even larger than Ba in BaFe$_2$As$_2$) results in a larger separation (7.0 Å) between Fe-Se layers than FeSe (5.5 Å). In our calculations, we used the experimental values of tetragonal lattice constants, $a=3.89$ Å and $c=14.00$ Å,[28] while the internal coordinate, z_{Se}, was relaxed by energy minimization [the atomic coordinates in this structure are Fe(4d) (0, 0.5, 0.25), Tl(2a) (0, 0, 0), and Se(4e)(0,0,z_{Se})]

The present calculations were performed within the generalized gradient approximation (GGA) of Perdew, Burke, and Ernzerhof (PBE),[29] using both the general potential linearized augmented plane-wave (LAPW) (Refs. 30 and 31) and projector augmented-wave (PAW) methods.[32,33] For the LAPW method, we employed LAPW spheres of radius $2.5a_0$ for Tl and $2.1a_0$ for Fe and Se. Well-converged basis sets with the size determined by $R_{Fe}k_{max}=8.0$ were used and semicore states of 5d for Tl, 3p for Fe, and 3d, 4s for Se
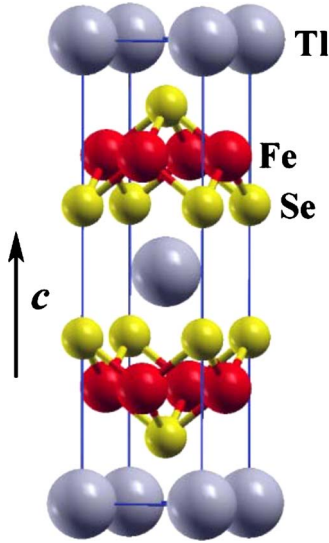
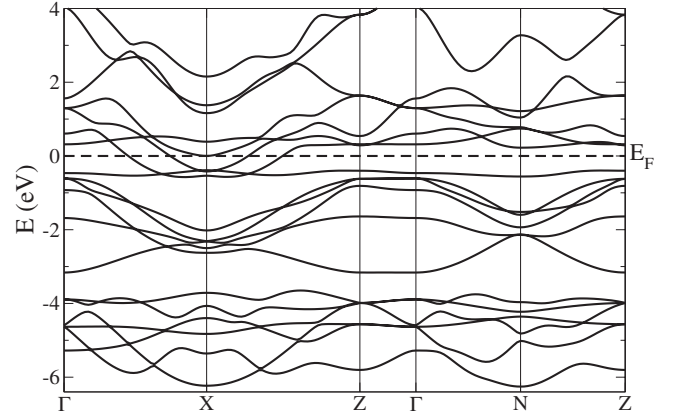FIG. 1. (Color online) Crystal structure of $ThCr_2Si_2$-type $TlFe_2Se_2$.

FIG. 2. Calculated electronic band structure of $TlFe_2Se_2$ with the checkerboard antiferromagnetic order, using the spin-polarized relaxed internal coordinate $z_{Se}=0.348$.

were included using local orbitals. In the PAW calculations, a kinetic-energy cutoff of 350 eV and augmentation charge cutoff of 511 eV were used. A $16\times16\times16$ grid was used for the body-centered tetragonal Brillouin-zone sampling in the self-consistent calculations, while more dense grids were used for density of states (DOS), Fermi surface, and especially magnetic calculations. The electric-field gradient (EFG) calculations were done with the all-electron LAPW method. The formation energy for vacancies was calculated with the PAW method using a 90 atom supercell, not including magnetism. The chemical potential of bulk elemental Tl was used as a reference. For bcc Fe our calculated PAW spin magnetic moment of $2.27\mu_B$ is in reasonable agreement with experimental value $2.12\mu_B$. Consistency between the LAPW and PAW calculations was carefully cross-checked and is indicated for example by very small residual forces for the relaxed structure, as well as very closely coincident band structures and density of states with two methods.

III. GROUND STATE: CHECKERBOARD ANTIFERROMAGNETISM

We begin with the magnetic order of stoichiometric $TlFe_2Se_2$, which is after all a known magnetic material. The energetics were calculated with optimization of the internal coordinate z_{Se} considering three different long-range magnetic orders possibly existing within Fe sheets:[15,34] ferromagnetism, nearest-neighbor checkerboard antiferromagnetism, and stripe antiferromagnetism (the pattern of the SDW in the undoped Fe superconductors). We found that the energy is always lowered in magnetic configurations where the Fe layer stacking along the c axis in antiferromagnetic, i.e., the interlayer Fe-Fe interaction, is antiferromagnetic. Relative to the non-spin-polarized case, we found a ferromagnetic instability (-44 meV/Fe) at the relaxed $z_{Se}=0.360$, with Fe moment $2.79\mu_B$/Fe. However a stronger instability is found for the checkerboard nearest-neighbor antiferromagnetic order

(-78 meV/Fe, $1.90\mu_B$/Fe) at relaxed $z_{Se}=0.348$, which is the ground state according to our calculations. This seems to be consistent with the only available experimental result, i.e., antiferromagnetism.[27] Obviously, further experiments will be helpful in confirming the magnetic order in $TlFe_2Se_2$. Interestingly, we did not find a magnetic instability at all for the SDW-like ordering. The sensitivity of the moment formation to the ordering pattern shows that the magnetism is itinerant in nature. In non-spin-polarized calculations, we obtain a relaxed optimal internal Se coordinate of $z_{Se}=0.342$, lower than both the experimental value 0.357 (with the difference of 0.2 Å) and the value obtained in calculations including magnetism. However, with the lowest-energy checkerboard order, we still obtain a value significantly lower than the experiment. In any case, considering also the difference between the ferromagnetic and checkerboard values of z_{Se} we do find the substantial magnetoelastic coupling, similar to the Fe-based superconducting phases.

The calculated band structure and electronic DOS with the ground-state checkerboard antiferromagnetic order are shown in Figs. 2 and 3, respectively. This material is metallic with two dispersive electron bands crossing the Fermi level (E_F) around the X point. As may be seen, the Fermi energy occurs in a trough in the DOS with a sharp peak ~0.5 eV below E_F. This peak arises from the very flat band below E_F, as seen in Fig. 2. At the Fermi energy, $N(E_F)=1.1$ eV^{-1} per Fe. The Fe $3d$ spin-down states are almost filled. Integration of partial spin states up to E_F and normalization with total Fe $3d$ states give 4.3 electrons in the majority states and 2.4 electrons in the minority states. This indicates the valence state of Fe is lower than $+2$ here. The Se p states are mainly found below -3 eV relative to the E_F, and are only modestly hybridized with Fe d states. The Tl $6s$ states are occupied, while the remaining Tl $6p$ states are above E_F, indicating that Tl occurs as monovalent Tl$^+$. This is consistent with electron doping of the Fe-Se sheets, by $0.5e$/Fe, i.e., nominal Fe valence of Fe$^{1.5+}$.

To connect with future experiments, we calculated the EFG of Fe and Se sites. These are defined as the second derivative of the Coulomb potential at the nuclear sites, and are probed by nuclear magnetic resonance (NMR) or nuclear
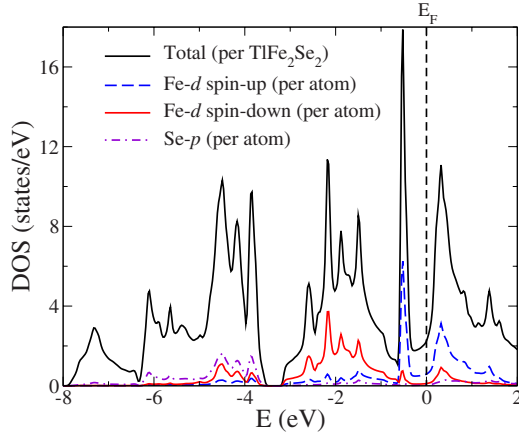
FIG. 3. (Color online) Calculated total and projected electronic DOS of TlFe$_2$Se$_2$ with the checkerboard antiferromagnetic order, using the LAPW method. For Fe, the minority half-filled (spin-up) and majority filled (spin-down) 3d states are shown separately.

quadrupole resonance (NQR) measurements. For tetragonal site symmetry, only the V_{zz} component is independent since the EFG tensor must be traceless. The calculated V_{zz} with the ground-state antiferromagnetic order are -2.2×10^{21} V/m^2 and -5.6×10^{21} V/m^2 for Fe and Se, respectively. As noted below, these values are very sensitive to the value of the internal coordinate, and therefore EFG measurements may be a very useful probe of magnetoelastic coupling in these materials. In this regard, it should be noted that Mukuda *et al.*[35] observed a relationship between the As quadrupole frequency and T_c in oxy-arsenides.

IV. RELATIONSHIP WITH THE IRON SUPERCONDUCTORS

To clearly show the relation of TlFe$_2$Se$_2$ with the Fe-based superconductors, we performed non-spin-polarized calculations of the electronic structure. The band structure, DOS, and Fermi surface are shown in Figs. 4–6, respectively. The main features of band structure show close similarity with that of FeSe (Ref. 18) and the Fe-based
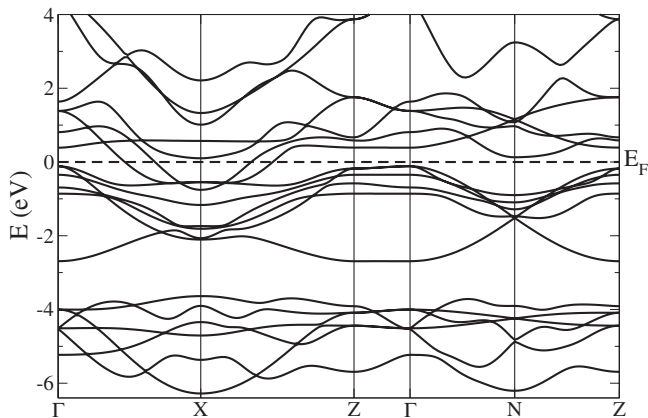

FIG. 4. Calculated non-spin-polarized band structure of TlFe$_2$Se$_2$ using the relaxed $z_{Se}=0.342$.

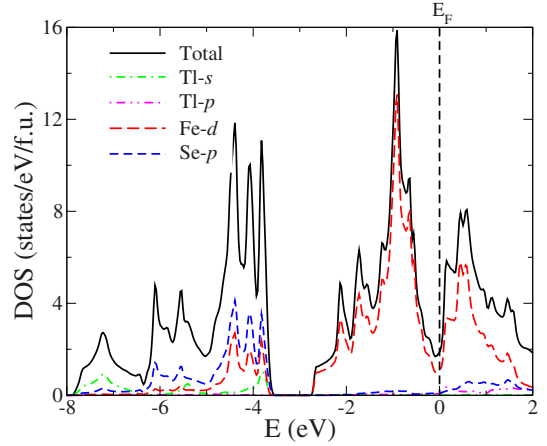

FIG. 5. (Color online) Calculated non-spin-polarized total and projected electronic DOS of TlFe$_2$Se$_2$. The values are on a per formula unit basis. Note that projections are onto the LAPW spheres, thus the absolute contributions of the Tl s and Se p states are underestimated owing to their more extended orbitals which extend significantly into the interstitial region.

arsenides.[36,37] In particular, the states near E_F are dominated by Fe d states (mainly derived from xz and yz orbitals) forming a pseudogap at the electron count of 6 (rather than 4 in the tetrahedral crystal-field scheme), with some mixture with Se p states. Tl occurs as Tl$^+$, as mentioned, with the Tl s states in the energy range ~-8 eV to -4 eV and the p-derived valence states are above E_F. The resulting doping relative to FeSe ($0.5e$/Fe) pushes E_F up from the steep lower edge of the pseudogap for FeSe (Ref. 18) to the bottom, leading to significantly decreased $N(E_F)$ of 0.92 eV^{-1} per Fe. As a result, the hole Fermi surfaces at the zone center in other Fe-based materials have completely disappeared and the electron sections at zone corner greatly expand, as shown in Fig. 6. This destroys the strong nesting between two-dimensional electron and hole Fermi surfaces in more lightly doped Fe-based materials and thus the SDW antiferromagnetic instability is suppressed.

As in the other Fe-based superconducting materials,[34] the non-spin-polarized electronic structure of TlFe$_2$Se$_2$ also shows great sensitivity to the Se height. For example, if the experimental $z_{Se}=0.357$ was used for calculations, $N(E_F)$ increases to 2.0 eV^{-1} per Fe though E_F still lies in the bottom
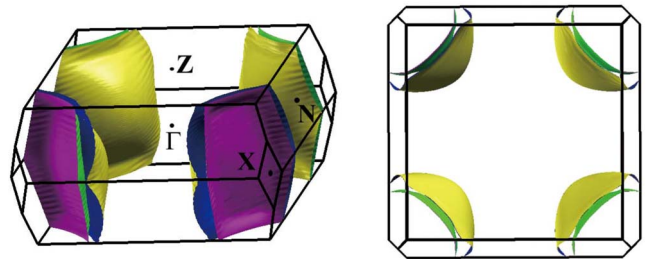

FIG. 6. (Color online) Calculated non-spin-polarized Fermi surface of TlFe$_2$Se$_2$. The right panels are top views along $Z-\Gamma$ direction. Here Fermi surfaces were mapped in the body-centered tetragonal Brillouin zone, and thus X point corresponds to the zone corner M point in the tetragonal Brillouin zone.

of pseudogap, and furthermore very small cylindrical hole Fermi surfaces appear at the zone center. This increase in $N(E_F)$ with z_{Se} provides an explanation for the fact that, although not the ground state, an itinerant ferromagnetic state is lower in energy than the nonmagnetic state even though the non-spin-polarized $N(E_F)$ (with the non-spin-polarized z_{Se}) is well below the Stoner criterion for itinerant magnetism.

The calculated V_{zz} of Fe and Se are 1.0×10^{21} V/m^2 and -4.4×10^{21} V/m^2 with experimental z_{Se} and -0.4×10^{21} V/m^2, and -5.2×10^{21} V/m^2 with relaxed z_{Se}, respectively. This illustrates the strong sensitivity of the EFG to the Se position, as mentioned above. Strong sensitivity of the EFG was also found for As in LaFeAsO by density functional calculations.[38]

V. SUMMARY AND DISCUSSION

To summarize, based on density functional calculations, we study magnetic properties, electronic structure, and relation to superconductivity for TlFe$_2$Se$_2$ occurring in the ThCr$_2$Si$_2$ structure. We find the nearest-neighbor checkerboard antiferromagnetism is the ground state, consistent with the available experimental data. The non-spin-polarized electronic structure of TlFe$_2$Se$_2$ shows close similarity with the Fe-based superconductors. Relative to those materials, Tl$^+$ is an electron dopant, donating 0.5 additional carrier per Fe relative to Fe-Se layers. This overdoping significantly enlarges the electron sections of Fermi surface at zone corner and eliminates hole sections at zone center, and thereby completely destroys the Fermi nesting and thus suppresses the SDW antiferromagnetic instability. We note that the compound crystallizes in the ThCr$_2$Si$_2$ structure, with a larger interlayer separation than FeSe. This might be favorable to superconductivity by empirically considering that the highest T_c so far is realized in the ZrCuSiAs-type compounds, i.e., the family with the largest interlayer space.[3,4] In any case, TlFe$_2$Se$_2$ is not reported to have excess Fe in interstitial sites whose moments may interact with superconducting Fe-Se planes and cause pair breaking. However, some Fe vacancies might form as the intrinsic defects in this system.[27,39] One natural way forward is via Tl deficiency, which would reduce the overdoping.

In order to evaluate this possibility, we calculated the formation energy of a Tl vacancy, using a supercell as described above. The calculated energy of -0.14 eV indicates metastability of the compound at low temperature, similar to PbZrO$_3$,[40,41] and that abundant Tl vacancies are very prone to form in this material. Thus, it may well be possible to produce Tl deficient material by modifying the growth conditions.[42] Owing to absence of excess Fe that cause pair breaking and suppress superconductivity in FeSe, if appropriate Tl deficiency is introduced, this material (Tl$_x$Fe$_2$Se$_2$) might be a good candidate for higher T_c in the chalcogenide family. This structure type may also provide an avenue for producing superconductivity in Fe-Te compounds, e.g., Tl$_x$Fe$_2$Te$_2$.

Even in the overdoped regime represented by TlFe$_2$Se$_2$, where the Fermi level has dropped into the bottom of the pseudogap, resulting in relatively low $N(E_F)$, we still found competing itinerant ferromagnetic and checkerboard antiferromagnetic states. In this regard, recent NMR experiments have shown evidence for pseudogap behavior in electron doped compounds (note this is the NMR pseudogap, not the pseudogap in the DOS), perhaps related to that in cuprates.[43,44] However, the behavior is different. In cuprates the pseudogap appears to be closely associated with the magnetic ordering of the undoped phases, and is seen most strongly in the underdoped regime. In contrast, the Fe-based superconductors show the pseudogap in the electron overdoped regime and not in the underdoped regime.[45,46] However, while Fe^{2+} is a common valence for Fe, Fe^{1+} is not and perhaps for this reason heavily overdoping beyond the superconducting regime while maintaining high sample quality has been difficult. Within an itinerant picture one may expect competition of SDW order and other magnetic (i.e., checkerboard) order in the Fe superconductors, which gives way to checkerboard order when the hole Fermi surface, and therefore the nesting, is destroyed by overdoping. Within such a scenario, and considering the experimental results, the pseudogap may be associated with incipient checkerboard order. In this regard, the chemical stability of TlFe$_2$Se$_2$ may provide a very useful window into the overdoped regime, especially if it can be chemically doped with holes, e.g., by Tl deficiency, as discussed above.

In fact, such studies might be particularly illuminating considering the phase diagram that is suggested by the present results in conjunction with the known phase diagrams of the electron-doped superconductors, first-principles results for them, and NMR data. In particular, without doping the materials show a spin-density wave, though with strongly reduced moments compared to standard density functional calculations. Such calculations do not include renormalization due to spin fluctuations—an effect that is small in most magnetic materials, such as Fe metal, but is apparently large in these materials. Electron (or hole) doping destroys the SDW, presumably by reducing the nesting between the hole and electron Fermi surfaces, in favor of a metallic state with evidence for strong spin fluctuations and superconductivity possibly related to spin fluctuations connected with the SDW. In this regime, there also appears to be a strong renormalization of magnetism, based on comparison of density functional results and experiment.[34,47] In general such renormalized states occur near quantum critical points or in situations where there is a competition between different magnetic orders. Considering the large composition range over which this behavior is seen, competition with another magnetic state may be crucial. The experimental observation that TlFe$_2$Se$_2$ is magnetic, and the likely checkerboard order suggest that the competing state in the superconducting phases might be the nearest-neighbor antiferromagnetic state. This state, although itinerant, is not driven by Fermi-surface nesting, and therefore nearness to it would be expected to yield spin fluctuations over a broader region of the Brillouin zone than nearness to a nesting driven SDW. While this would make them more effective in renormalizing the SDW instability due to the larger phase space for competing fluctuations, it would also make them harder to observe by inelastic neutron scattering as compared to the nest-

ing related fluctuations. Nonetheless, it would be of great interest first of all to confirm experimentally that the ground state of $TlFe_2Se_2$ is the checkerboard state, and second to study the overdoped regime, perhaps using this chemistry, to relate spin fluctuations from neutron scattering and the NMR pseudogap. Furthermore, it will be of considerable interest to study the interplay between superconductivity and the onset of checkerboard order, if this in fact is established at high doping. While the SDW and superconductivity mediated by nesting related spin fluctuations would compete for the same electrons at the Fermi surface, this is not necessarily the case for the checkerboard order, and so some difference may be anticipated from the behavior at the underdoped antiferromagnetic SDW-superconducting boundary, perhaps including coexistence of the two orders over some composition range.

[1] Y. Kamihara, H. Hiramatsu, M. Hirano, R. Kawamura, H. Yanagi, T. Kamiya, and H. Hosono, J. Am. Chem. Soc. **128**, 10012 (2006).

[2] Y. Kamihara, T. Watanabe, M. Hirano, and H. Hosono, J. Am. Chem. Soc. **130**, 3296 (2008).

[3] C. Wang *et al.*, EPL **83**, 67006 (2008).

[4] G. Wu, Y. Xie, H. Chen, M. Zhong, R. Liu, B. Shi, Q. Li, X. Wang, T. Wu, Y. Yan, J. Ying, and X. Chen, J. Phys.: Condens. Matter **21**, 142203 (2009).

[5] M. Tegel, S. Johansson, V. Weiss, I. Schellenberg, W. Hermes, R. Pöttgen, and D. Johrendt, EPL **84**, 67007 (2008).

[6] S. Matsuishi, Y. Inoue, T. Nomura, M. Hirano, and H. Hosono, J. Phys. Soc. Jpn. **77**, 113709 (2008).

[7] M. Rotter, M. Tegel, and D. Johrendt, Phys. Rev. Lett. **101**, 107006 (2008).

[8] X. C. Wang, Q. Q. Liu, Y. X. Lv, W. B. Gao, L. X. Yang, R. C. Yu, F. Y. Li, and C. Q. Jin, arXiv:0806.4688 (unpublished).

[9] D. R. Parker, M. J. Pitcher, and S. J. Clarke, arXiv:0810.3214 (unpublished).

[10] F.-C. Hsu *et al.*, Proc. Natl. Acad. Sci. U.S.A. **105**, 14262 (2008).

[11] Y. Mizuguchi, F. Tomioka, S. Tsuda, T. Yamaguchi, and Y. Takano, Appl. Phys. Lett. **93**, 152505 (2008).

[12] C. de la Cruz *et al.*, Nature (London) **453**, 899 (2008).

[13] M. Rotter, M. Tegel, D. Johrendt, I. Schellenberg, W. Hermes, and R. Pöttgen, Phys. Rev. B **78**, 020503(R) (2008).

[14] M. S. Torikachvili, S. L. Bud'ko, N. Ni, and P. C. Canfield, Phys. Rev. Lett. **101**, 057006 (2008).

[15] I. I. Mazin, D. J. Singh, M. D. Johannes, and M. H. Du, Phys. Rev. Lett. **101**, 057003 (2008).

[16] M. A. McGuire *et al.*, Phys. Rev. B **78**, 094517 (2008).

[17] H. H. Klauss *et al.*, Phys. Rev. Lett. **101**, 077005 (2008).

[18] A. Subedi, L. Zhang, D. J. Singh, and M.-H. Du, Phys. Rev. B **78**, 134514 (2008).

[19] R. Yoshida, T. Wakita, H. Okazaki, Y. Mizuguchi, S. Tsuda, Y. Takano, H. Takeya, K. Hirata, T. Muro, M. Okawa, K. Ishizaka, S. Shin, H. Harima, M. Hirai, Y. Muraoka, and T. Yokoya, J. Phys. Soc. Jpn. **78**, 034708 (2009).

[20] K. Yeh, T. Huang, Y. Huang, T. Chen, F. Hsu, P. Wu, Y. Lee, Y. Chu, C. Chen, J. Luo, D. Yan, and M. Wu, arXiv:0808.0474 (unpublished).

[21] M. H. Fang, H. M. Pham, B. Qian, T. J. Liu, E. K. Vehstedt, Y. Liu, L. Spinu, and Z. Q. Mao, Phys. Rev. B **78**, 224503 (2008).

[22] W. Bao, Y. Qiu, Q. Huang, M. Green, P. Zajdel, M. Fitzsimmons, M. Zhernenkov, M. Fang, B. Qian, E. Vehstedt, J. Yang, H. Pham, L. Spinu, and Z. Mao, arXiv:0809.2058 (unpublished).

[23] S. Li, C. Delacruz, Q. Huang, Y. Chen, J. Lynn, J. Hu, Y. Huang, F. Hsu, K. Yeh, M. Wu, and P. Dai, Phys. Rev. B **79**, 054503 (2009).

[24] Y. Mizuguchi, F. Tomioka, S. Tsuda, T. Yamaguchi, and Y. Takano, Appl. Phys. Lett. **94**, 012503 (2009).

[25] L. Zhang, D. J. Singh, and M.-H. Du, Phys. Rev. B **79**, 012506 (2009).

[26] M. H. Fang, B. Qian, H. M. Pham, J. H. Yang, T. J. Liu, E. K. Vehstedt, L. Spinu, and Z. Q. Mao, arXiv:0811.3021 (unpublished).

[27] L. Häggström, H. R. Verma, S. Bjarman, R. Wäppling, and R. Berger, J. Solid State Chem. **63**, 401 (1986).

[28] K. Klepp and H. Boller, Monatsh. Chem. **109**, 1049 (1978).

[29] J. P. Perdew, K. Burke, and M. Ernzerhof, Phys. Rev. Lett. **77**, 3865 (1996).

[30] P. Blaha, K. Schwarz, G. Madsen, D. Kvasnicka, and J. Luitz, *An Augmented Plane Wave + Local Orbitals Program for Calculating Crystal Properties* (K. Schwarz, Technical University, Wien, Austria, 2001).

[31] D. J. Singh and L. Nordstrom, *Planewaves Pseudopotentials and the LAPW Method*, 2nd ed. (Springer, Berlin, 2006).

[32] G. Kresse and D. Joubert, Phys. Rev. B **59**, 1758 (1999).

[33] G. Kresse and J. Furthmüller, Phys. Rev. B **54**, 11169 (1996).

[34] I. I. Mazin, M. D. Johannes, L. Boeri, K. Koepernik, and D. J. Singh, Phys. Rev. B **78**, 085104 (2008).

[35] H. Mukuda *et al.*, J. Phys. Soc. Jpn. **77**, 093704 (2008).

[36] D. J. Singh and M. H. Du, Phys. Rev. Lett. **100**, 237003 (2008).

[37] D. J. Singh, Phys. Rev. B **78**, 094511 (2008).

[38] H.-J. Grafe, G. Lang, F. Hammerath, D. Paar, K. Manthey, K. Koch, H. Rosner, N. Curro, G. Behr, J. Werner, N. Leps, R. Klingeler, and B. Buchner, New J. Phys. **11**, 035002 (2009).

[39] H. Sabrowsky, M. Rosenberg, D. Welz, P. Deppe, and W. Schäfer, J. Magn. Magn. Mater. **54-57**, 1497 (1986).

[40] E. Takayama-Muromachi and A. Navrotsky, J. Solid State Chem. **72**, 244 (1988).

[41] R. Kagimura and D. J. Singh, Phys. Rev. B **78**, 174105 (2008).

[42] Since the negative formation energy of Tl vacancies corresponds to metastability of the compound, we also checked the heat of formation for $TlFe_2Se_2$ in terms of elements. The obtained value is -1.02 eV/f.u. (98 kJ/mol/f.u.), which indicates it is at least stable against decomposition into elements.

[43] W. W. Warren, Jr., R. E. Walstedt, G. F. Brennert, R. J. Cava, R. Tycko, R. F. Bell, and G. Dabbagh, Phys. Rev. Lett. **62**, 1193 (1989).

[44] H. Alloul, T. Ohno, and P. Mendels, Phys. Rev. Lett. **63**, 1700 (1989).

[45] Y. Nakai, K. Ishida, Y. Kamihara, M. Hirano, and H. Hosono, J. Phys. Soc. Jpn. **77**, 073701 (2008).

[46] F. Ning, K. Ahilan, T. Imai, A. S. Sefat, R. Jin, M. A. McGuire, B. C. Sales, and D. Mandrus, J. Phys. Soc. Jpn. **77**, 103705 (2008).

[47] D. J. Singh, arXiv:0901.2149 (unpublished).

[48] A. Kokalj, J. Mol. Graphics Modell. **17**, 176 (1999).